Field Precision LLC

Simulating a planar electron-beam gun

Stanley Humphries, Ph.D.

Figure 1: Electron gun assembly.

1 Gun simulation mesh and electrostatic field calculation

Planar electron beams have potential application to high-power microwave sources. The beam shape reduces space-charge forces and consequent beam energy spread for a given current. The design challenge is that planar-beam guns require a complete three-dimensional analysis. In this report I describe benchmark calculations that illustrate setup techniques for the **OmniTrak** code. The work was carried out for Prof. N. Luhmann at the University of California at Davis. The calculations address the the electron gun and periodic-permanent magnet transport system described in the report G. Scheitrum, *Design and Construction of a W-band Sheet Beam Klystron* (Stanford Linear Accelerator Center, SLAC-PUB-11688, 2005). Figure 1 shows the gun assembly with the end-flange, shaped anode and transport tube removed. The goal is to produce a planar beam with short dimension (x) along the short direction of the shaped focusing electrode and long dimension (y) along the long direction. The circular cathode is slightly convex. The surface depression has cylindrical symmetry about an axis parallel to the long dimension.

The first task was to create a three-dimensional mesh: introducing geo-
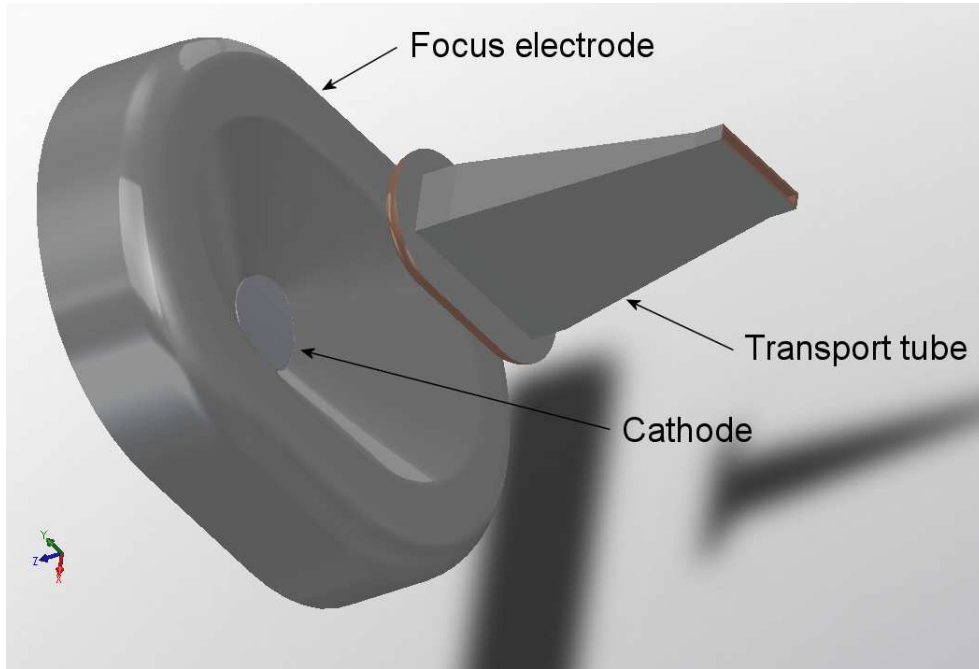
Figure 2: **SolidWorks** view of assembly parts with complex shapes.

metric information into **MetaMesh** and making a good choice of element sizes. A completed three-dimensional data set in **SolidEdge** format prepared at the Stanford Linear Accelerator Center was available. The assembly parts were abstracted and simplified at UCD. The intention was to include only parts that affected beam dynamics and to remove unnecessary details like hidden bolt holes. The information was exported in IGES file so that I could transfer it to **SolidWorks**. I decided that the most effective approach would be to use STL model import for the parts with complex shapes: the focus electrode, cathode and the transport tube with shaped anode. The simple *Cylinder* model in **MetaMesh** could be used for the other parts: the end flange, vacuum chamber interior and cathode support.

Figure 2 shows a **SolidWorks** visualization of the complex parts. I used the *Save as* command, choosing a fine facet resolution in the STL mode. The program created individual STL files for the cathode, focus electrode and top and bottom sections of the transport tube. The facets preserved their absolute locations in the assembly space. The dimensions in the files I received were in inches and the point $z = 0.0$" was just downstream from the inner surface of the end flange. The axial location of the exit of the transport tube was $z = 0.733$".

The system had symmetry about the planes $x = 0.0$" and $y = 0.0$". To minimize run times, I limited the calculation to the first quadrant of the x-y plane. I was able to use the full STL models because **MetaMesh**

3

automatically clips parts at the boundary of the solution volume. There are several features of interest in the **MetaMesh** input file `PLANARGUN.MIN`:

The gap between the cathode and focusing electrode was narrow. The cathode had outer radius 0.125" while the inner radius of the focusing electrode was 0.130". To define a good cathode edge, I used a mesh size of 0.0025" over the x-y plane out to the inner radius of the focusing electrode. The element size was 0.005" to the outer radius of the focus electrode and 0.025" over the bulk of the vacuum volume. The resolution along x was defined in the script by:

```
XMesh
    0.0000E+00  1.2500E-01  2.5000E-03
    1.2500E-01  1.3000E-01  2.5000E-03
    1.3000E-01  2.2000E-01  5.0000E-03
    2.2000E-01  1.2750E+00  2.5000E-02
End
```

The element size in z was small near the cathode surface. I defined a resolution zone boundary at $z = -0.0325$", the location of the inner face of the end flange. This provision ensured that a plane of the foundation mesh was at this position, helping **MetaMesh** represent the large flat surface.

```
ZMesh
    -1.5000E+00 -9.0000E-01  5.0000E-02
    -9.0000E-01 -8.2000E-01  2.5000E-02
    -8.2000E-01 -8.0670E-01  2.5000E-03
    -8.0670E-01 -7.8000E-01  2.5000E-03
    -7.8000E-01 -4.2500E-01  2.5000E-02
    -4.2500E-01 -3.2500E-02  1.0000E-02
    -3.2500E-02  7.3300E-01  2.5000E-02
End
```

The vacuum region (`VACUUM`) was a cylinder carved out of the grounded vacuum chamber wall (`GROUND`), which initially filled the entire solution volume. The `COAT` statement ensured that the shared nodes between the regions had the fixed potential condition:

```
PART
  Region: VACUUM
  Name: VACUUM
  Type: Cylinder
  Fab:   1.2300E+00  1.5000E+00
  Shift:   0.0000E+00  0.0000E+00 -7.8250E-01
  Surface Part VChamber
  Coat Ground Ground
END
```

The part EMITDEF was a cylinder with the same radius as the cathode that covered the axial region occupied by the concave surface. The part (with the physical property of vacuum) had its own region designation (EMITDEF). When the cathode was inserted, it over-wrote a portion of the region. The EMITDEF elements were used to identify the emission nodes on the cathode surface.

```
PART
  Region: EMITDEF
  Name: EMITDEF
  Type: Cylinder
  Fab: 0.123 0.0200
  Shift: 0.00 0.00 -0.800
  Surface Region Vacuum
END
```

The shape of the part representing the anode and transport tube was defined by the facets of an STL file. In the following listing, note the presence of the ROTATE command. As supplied, the IGES assembly would create a beam moving in the $-z$ direction. The 180º rotation about x of all STL parts gave a beam that moved in the positive $+z$ direction.

```
PART
  Region: GROUND
  Name: Anode
  Type: STL  output_dn  Fit
  Fab:   8.0000E-01  3.0000E-01
  Rotate:   180.00    0.00    0.00  XYZ
  Surface Region Vacuum
END
```

The cathode was defined by an `STL` file with a 180° rotation and a relatively tight fitting tolerance (0.95) to produce a good edge. The `COAT` command set nodes on the surface adjacent to the `EMITDEF` to a special emission region (`EMIT`).

```
PART
  Region: Cathode
  Name: Cathode
  Type: STL  cathode  Fit
  Fab:   9.5000E-01  3.0000E-01
  Rotate:  180.00    0.00    0.00  XYZ
  Surface Region EmitDef
  Surface Region Vacuum
  Coat EmitDef Emit
END
```

MetaMesh required about 5 minutes to produce a mesh with 1,713,040 elements. The input file for the **HiPhi** solution was straightforward. The `VACUUM` and `EMITDEF` regions were dielectrics with $\epsilon_r = 1.0$. The `GROUND` region had the fixed potential $\phi = 0.0$ V while the `CATHODE` and `EMIT` regions were at potential $\phi = -74.0$ kV. The initial electrostatic solution took about 27 minutes.

2 Gun electron dynamics

The next step was the **OmniTrak** solution for the electron beam. Calculations of beam-generated magnetic fields involve significant labor. Because relativistic effects at 74 keV represent a perturbation, I performed the calculation in two stages to minimize the run time.

An initial calculation without magnetic fields gave the self-consistent electric field distribution near the cathode. The electric field in this region constrained the model particle currents which were almost independent of beam-generated magnetic field.

A second relativistic calculation fine-tuned the orbits of extracted electrons. The self-consistent electric field from the first solution was used as input so that only a few iteration cycles were necessary.

Table 1 shows the input file for the first calculation. The **HiPhi** solution (with dimensions in inches) was loaded. Beam tracking was performed in the *SCharge* mode which includes self-consistent beam-generated electric fields but no magnetic field. Model electrons were emitted from the region `EMIT`

Table 1: Input file `PLANARGUNNR.OIN`

```
FIELDS
  EFIELD3D: PLANARGUN.HOU
  DUNIT:   39.37
  MAXCYCLE(E):    350
  RESTARGET(E):   2.0000E-07
END
PARTICLES SCHARGE
  NCYCLE:   10
  AVG(E):   4.0000E-01
  EMIT(5):   0.0000E+00 -1.0000E+00  0.00375  1
  REFLECTPLANE YDn 0.0
  REFLECTPLANE XDn 0.0
  EDIRECT Field
END
DIAGNOSTICS
  PARTFILE: PLANARGUNNR
  EDUMP: PLANARGUNNR.HOU
  PARTLIST
END
ENDFILE
```

with a standoff distance of 0.00375" (about 1.5 times the local axial element length). A single model electron was created at the center of each facet of the emission surface. Particle reflection planes were defined at $x = 0.0$" and $y = 0.0$". In response to the command `EDIRECT EFIELD`, the program set direction vectors for particles at the emission surface parallel to the local electric field. This provision avoided the effects of small distortions of emission facets at the cathode edge. The `EDUMP` command called for a record of the self-consistent electric field distribution after 10 iteration cycles. A total of 2092 model electrons were created. The converged solution required about 31 minutes. The emitted current for a quadrant was 0.783 A, giving a total current of 3.131 A. The value was below the design current of 3.5 A determined by the **Michelle** code, but was consistent with experimental measurements.

Table 2 shows the input file for the second calculation. There were several difference from the first run:

The `EFIELD3D` command directed the program to load the electric field from the previous solution.

The run employed the `RELBEAM` mode, which included calculation of

7

the beam-generated field and its effect on electron dynamics.

The `SUPPRESS` command removed correction factors for the emitted current to minimize initial solution oscillations. Adjustments were not necessary because the initial particle currents started close to their final values.

I picked the mesh for the computation of the beam-generated magnetic field (`BBMESH` command) to encompass the volume in x-y-z space occupied by the beam. The element sizes provided good resolution near the beam focus.

The `BBELEM` command set minimum values for the size of current elements to compute the magnetic field. The minimum length was 0.15". small compared to the axial distance for changes in the beam profile. The radius of 0.005" provided effective transverse smoothing without loosing resolution of the beam edge.

The `BBSYMPLANE` commands signal that the calculation was to be performed in one quadrant. In response, **OmniTrak** includes contributions from virtual particles in the other three quadrants.

The calculation ran about 63 minutes. As expected, the total emitted current had only a small variation between the cycles. The final value of 3.11 A was close to that of the non-relativistic calculation.

Figure 3 is a three-dimensional view of beam solution. Figure 4, a two-dimensional slice, illustrates beam dynamics in the long direction. The figure includes equipotential lines in the plane $x = 0.0$" with model electron orbits projected to the plane. The initial focusing near the source counteracted the lens effect at the exit aperture to produce a relatively parallel beam. A phase-space plot of y-y' at the end of transport tube showed that the beam was expanding with an envelope angle of $+0.46^\circ$. Figure 5 shows particle orbits in the short direction. The distribution approached a waist point at the transport tube exit. Finally, Fig. 6 shows the shape of the beam spot at the exit of the transport tube.

I used **GenDist** to find quantitative information on the exit distribution. I loaded the file `PLANARGUNR.PRT` created by the second **OmniTrak** run. Figure 7 shows the marginal probabilities $F(x)$ and $F(y)$. The beam was well-localized in the short direction with a low-density halo. In the long direction, the line current approximated a cosine distribution as expected in a linear transformation of a circle to an ellipse. The exit beam aspect ratio was about 20:1.

Table 2: Input file `PLANARGUNR.OIN`

```
FIELDS
  EFIELD3D: PLANARGUNNR.HOU
  DUNIT:   39.37
  MAXCYCLE(E):    350
  RESTARGET(E):   2.0000E-07
END
PARTICLES RELBEAM
  NCYCLE:   7
  AVG:   4.0000E-01
  EMIT(5):    0.0000E+00 -1.0000E+00  0.00375  1
  REFLECTPLANE YDn 0.0
  REFLECTPLANE XDn 0.0
  EDIRECT Field
  SUPPRESS 1.0 1.0 1.0 1.0 1.0
  BBMESH  0.000 0.125  25  0.000  0.150  20  -0.810   0.733  30
  BBELEM 0.150  0.005
  BBSYMPLANE X
  BBSYMPLANE Y
END
DIAGNOSTICS
  PARTFILE: PLANARGUNR
  EDUMP: PLANARGUNR.HOU
  BBDUMP: PLANARGUNR.GOU
  PARTLIST
END
ENDFILE
```
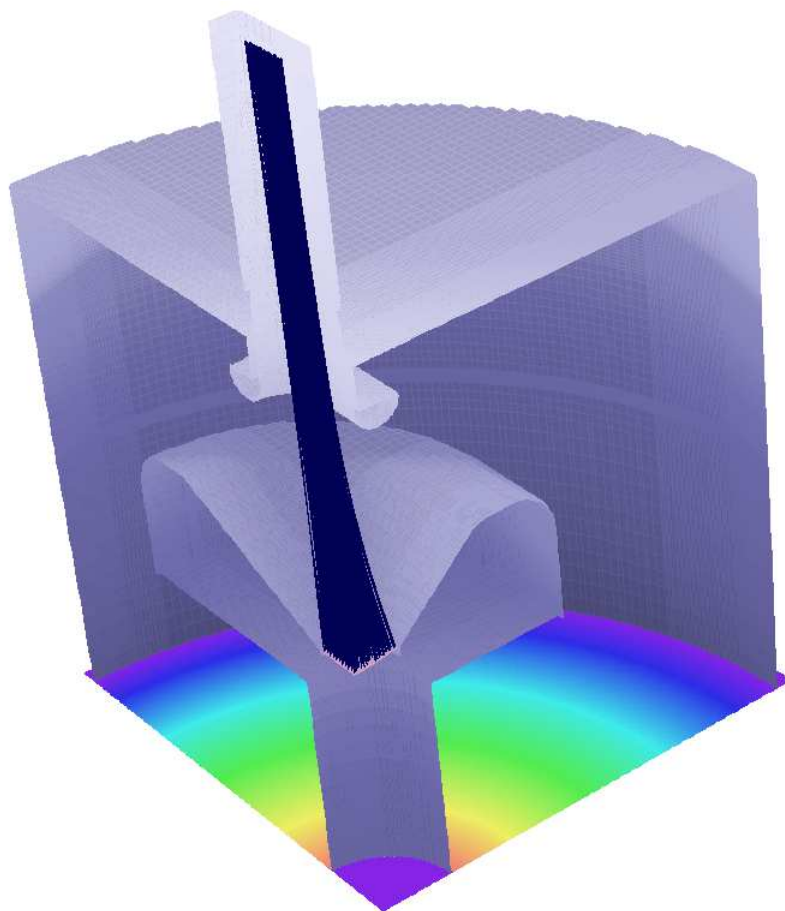
Figure 3: Three-dimensional view of the relativistic beam solution.
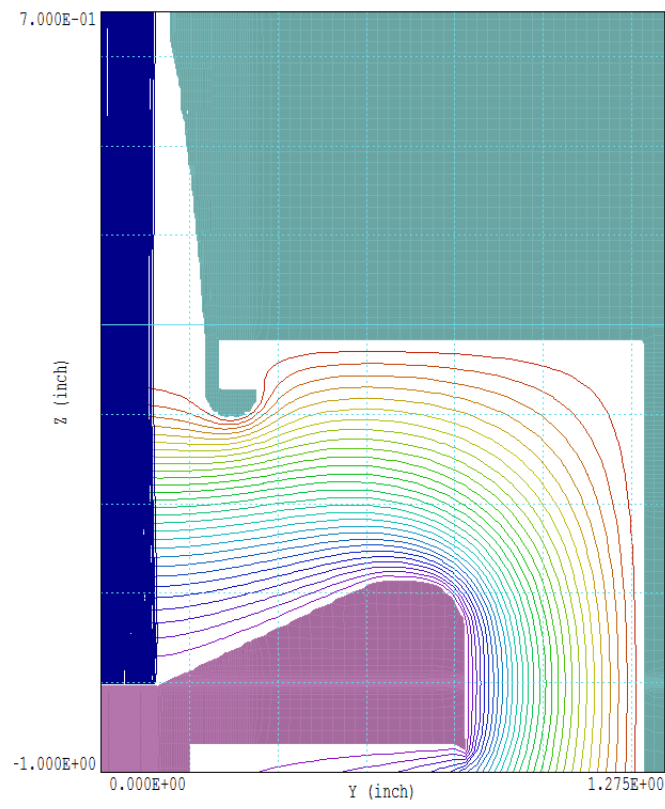
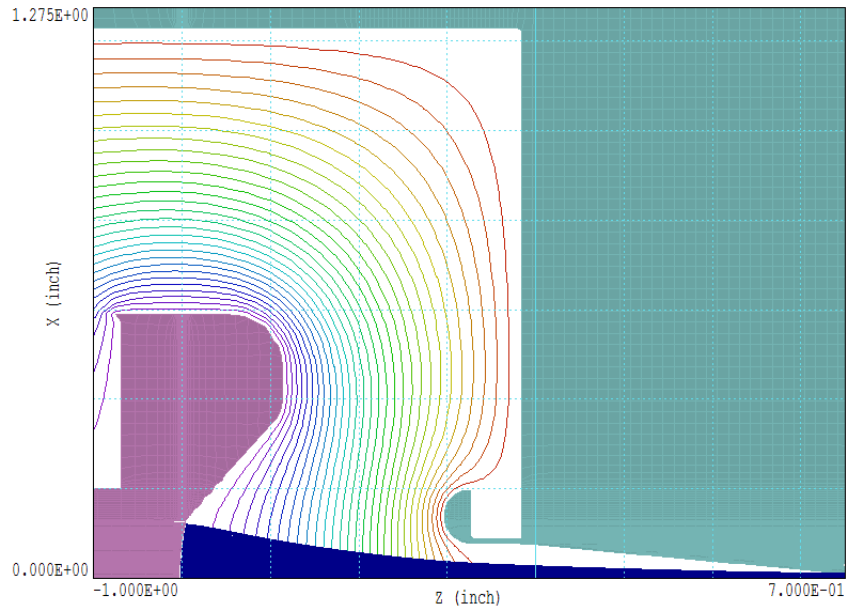Figure 4: Projected particle orbits in the long direction with the field distribution at $x = 0.0$.

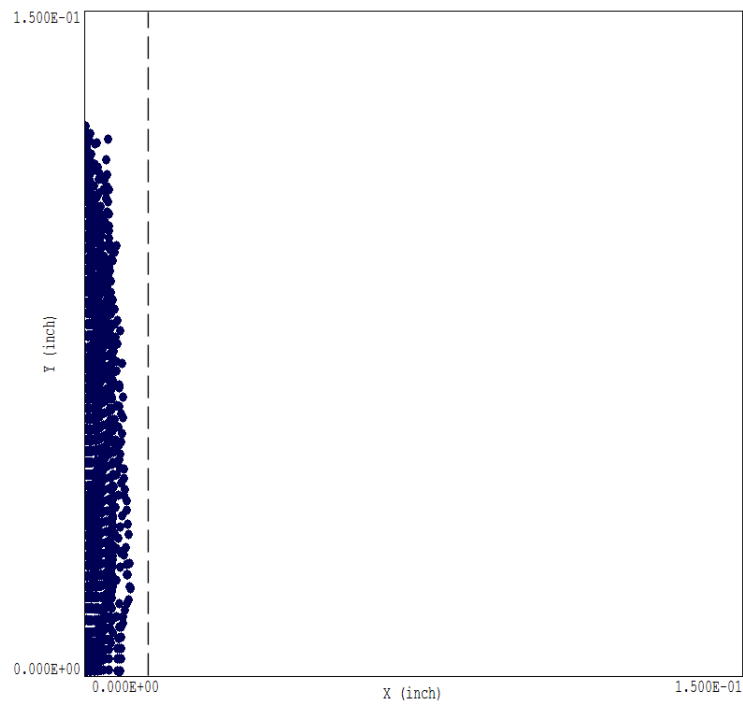Figure 5: Projected particle orbits in the short direction with field distribution at $y = 0.0$.

Figure 6: Distribution of model particles in the plane $z = 0.773$" at the exit of the transport tube. The dashed line shows the position of the transport tube wall.
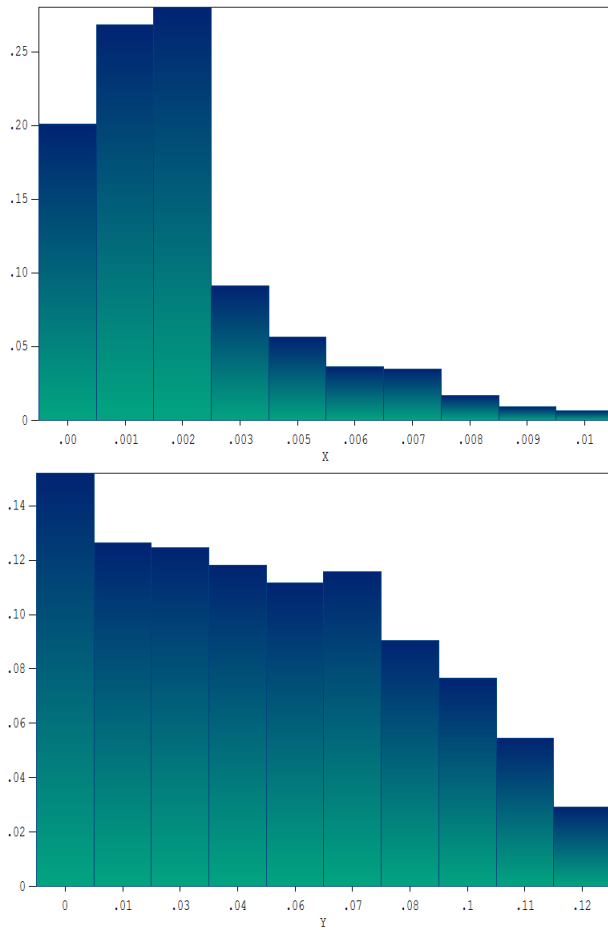
Figure 7: Beam distributions at the exit of the transport tube ($z = 0.773$"). Top: $F(x) = \int dy f(x, y)$. Bottom: $F(y) = \int dx f(x, y)$.
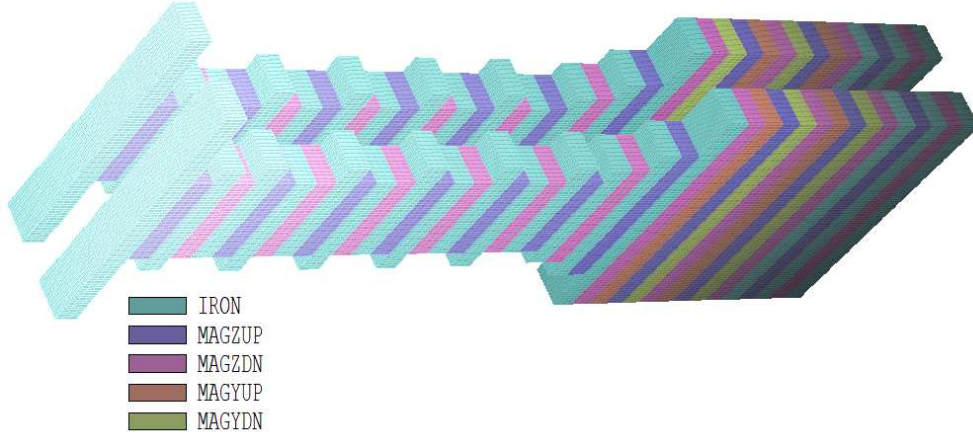
Figure 8: Periodic-permanent-magnet assembly.

3 Periodic-permanent-magnet transport system

The microwave system utilizes a periodic-permanent-magnet system of length 120 mm to maintain the dimensions of the planar beam through a klystron structure. Figure 8 is a three-dimensional view of the system. I set the axial coordinate axis ($z = 0.0$ mm) at the entrance face of the first pole. The assembly contained 34 iron pole pieces, 20 magnets magnetized in $+z$, 20 in $-z$, 8 in $+x$ and 8 in $-x$. The gap between the upper and lower sections was 5.56 mm. All pieces had a cross-section dimension of 5.51 mm in x by 3.00 mm in z with varying lengths in the long direction (y). Some of the poles were offset in y to provide focusing forces in the long direction. Because of the offsets, the structure did not have a symmetry plane. As a result, it was necessary to model the complete structure.

The file `MAGNET.MIN` described the system geometry. I set up the mesh with ample space around the magnets to check the fringe-field strength, particularly in the transport tube region. All parts of the assembly could be represented by the **MetaMesh** *Box* model. I set resolution boundaries in the x direction so that the foundation mesh had planes at the top and bottom of the poles and magnets for an accurate representation of the volumes. The resolution definition in the y direction ensured foundation-mesh planes that corresponded exactly with the ends of the pieces. In the beam propagation volume, the element size was 0.20 mm in the x and y directions. I found that an axial element size of 0.50 mm was necessary for accurate field interpolations and orbit calculations. The final mesh had 3,262,464 elements. The Magnum calculation was controlled by the file `MAGNET.GIN`. The permanent-
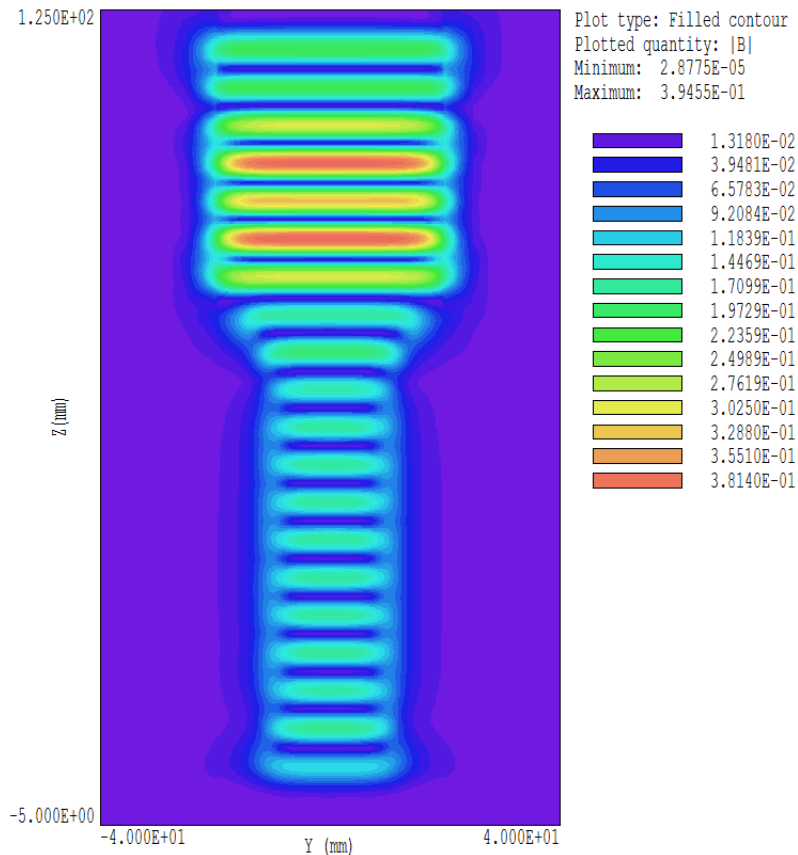
Figure 9: Variation of $|B_z|(y, z)$ in the plane $x = 0.0$.

magnet materials had a remanence field of 0.91 tesla. The time to calculate fields in the air and iron regions was about 2.5 hours.

Figure 9 is a filled-contour plot of $|B_z|$ over the short-direction midplane ($x = 0.0$ mm). Figure 10 shows a scan of $B_z(z)$ along the axis ($x = 0.0$ mm, $y = 0.0$ mm). The results were in good agreement with independent calculations performed at UCD using both **Magnum** and **Maxwell3D**.

4   Transport calculations

The final task was to confirm that the magnet stack could contain the focused beam distribution throughout its length. The transportation calculation was performed independently because it would have been quite inefficient to combine it with the gun simulation. It was important to start particles at a point outside the stack where $B_z \cong 0.0$ to ensure that they entered with zero canonical momentum P_y. Fortunately, the field was well-localized. I found that B_z dropped to only about 0.1% of its peak value at $z = -5.0$ mm.
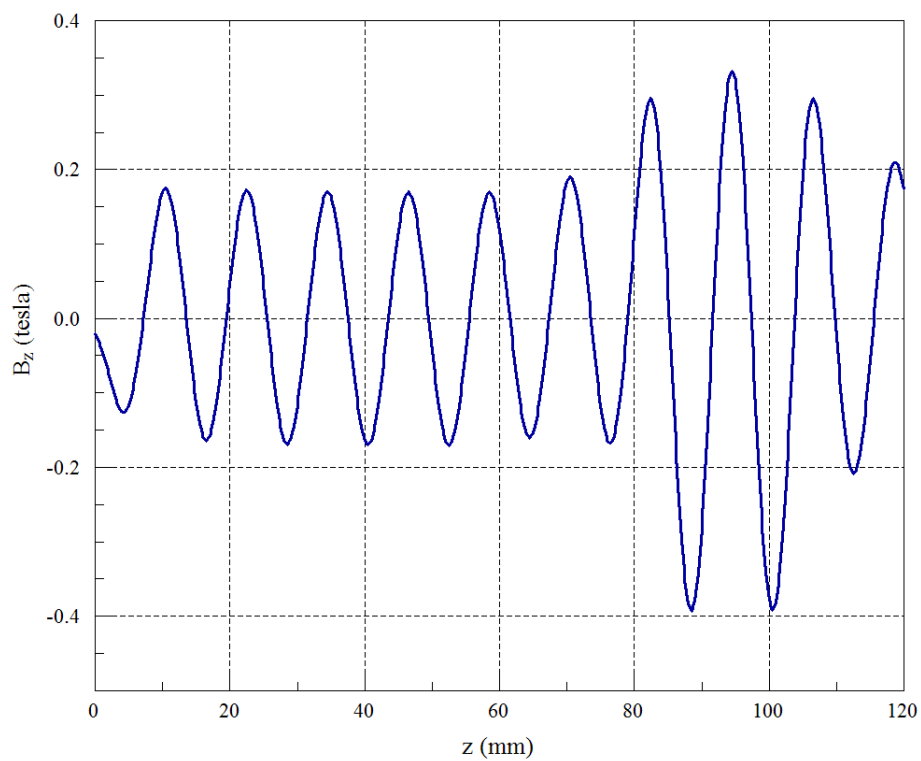
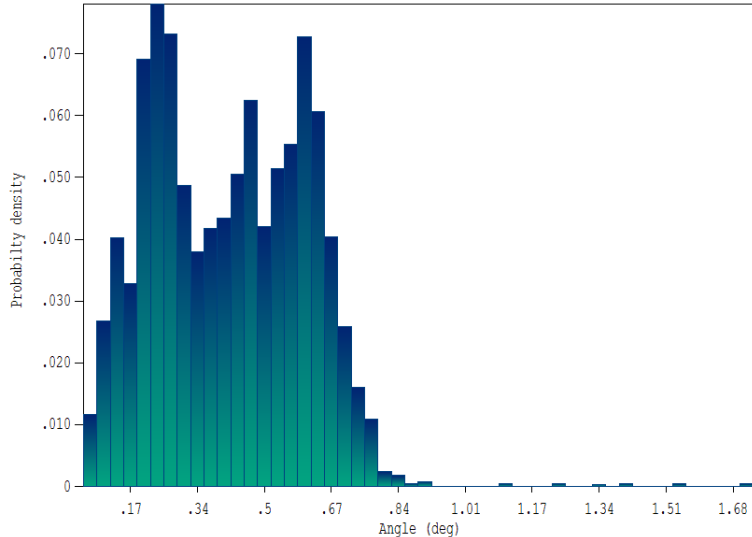Figure 10: Variation of $B_z(z)$ at $x = 0.0$ mm, $y = 0.0$ mm.

Figure 11: Electron distribution as a function of short-direction angle, results from the gun calculation of Sect. 2.

I used the field solution described in Sect. 3 as input to **OmniTrak**. In an initial calculation, I tracked single-particle orbits to check validity and accuracy. I started electrons with kinetic energy 74 keV at several different displacements in x and y. Using my original magnetic field solution with an axial element size of 1.0 mm, I observed some growth of transverse oscillations and discontinuities in axial field scan. With a reduced element length of 0.5 mm, I observed stable orbits with good energy conservation. Figure 10 shows a field scan with the fine mesh.

I proceeded to transport calculations with full beam distributions and self-consistent effects of beam-generated fields. Because there were no applied electric fields and the paraxial beam was approximately monoenergetic, it was sufficient to use the `RELAPPROX` command in the `SCHARGE` mode. In this case, **OmniTrak** calculated only beam-generated electric fields and then divided by a factor $1/\gamma^2$ to determine transverse forces. I used two approaches for demonstration calculations. In the first, I employed **GenDist** to create a distribution based on data from the gun simulation (Sect. 2). Figure 11 shows the angular distribution $f(x')$ from the gun calculation. The **GenDist** input file is shown in Table 3. In response, the program generated a `PRT` file that contained 2500 electrons with kinetic energy 74.0 keV. The electrons started at $z = -5.0$ mm. The 3.1 A beam had full widths of 0.3 mm in x and 6.0 mm in y. There was a weighted distribution of angle in the short direction that extended over the range $x' = \pm 0.7º$.

An electrostatic mesh was necessary to record beam space-charge and to calculate the beam-generated electric field (`CHAMBER.MIN`). I created a solu-

Table 3: GenDist input file PLANAR_INPUT.DST

```
FileType = PRT
RestMass =    0.0000E+00
Charge =    -1.0000E+00
Energy =    7.4000E+04
Def(Rect) =    0.15   3.00     50      50
Shift = 0.00 0.00 -5.00
Distribution = Uniform
Current = 3.1
DxDist
  -0.7  0.00
  -0.6  0.27
  -0.5  0.49
  -0.4  0.67
  -0.3  0.82
  -0.2  0.92
  -0.1  0.98
  -0.0  1.00
   0.1  0.98
   0.2  0.92
   0.3  0.82
   0.4  0.67
   0.5  0.49
   0.6  0.27
   0.7  0.00
End
EndFile
```

Table 4: Input file `TRANSPORT01.OIN`

```
FIELDS
  EFIELD3D: CHAMBER.HOU
  BFIELD3D: MAGNET.GOU
  DUNIT:   1.0000E+03
  MAXCYCLE:    500
  RESTARGET:   5.0000E-07
END
PARTICLES SCHARGE
  NCYCLE:     8
  AVG:   6.0000E-01
  PFILE: PLANAR_INPUT
  RELAPPROX
  DT: 2.0E-12
END
DIAGNOSTICS
  PARTFILE: TRANSPORT01
  EDUMP: TRANSPORT01.HOU
  PARTLIST
END
ENDFILE
```

tion with boundaries equal to those of the apertures of the klystron structure. It extended over the range -0.35 mm $\leq x \leq$ 0.35 mm, -4.0 mm $\leq x \leq$ 4.0 mm, -6.0 mm $\leq x \leq$ 124.0 mm. The solution volume had the properties of vacuum with grounded boundaries at x_{min}, x_{max}, y_{min} and y_{max} (`CHAMBER.HIN`). The input file for the **OmniTrak** run is shown in Table 4. In response, the program loaded the files `CHAMBER.HOU` (dummy electric field solution to record beam-generated electric field), `MAGNET.GOU` (magnetic field solution from Sect. 3) and `PLANAR_BEAM.PRT` (input particle distribution created by **GenDist**). The `PARTICLES` section specified the `SCHARGE` mode using the relativistic approximation with eight iteration cycles to find the self-consistent electric field.

Figure 12 shows particle orbits through the entire axial length projected to the x-y plane. The beam was well-contained in the short direction with 100% transmission through the chamber. The plot also shows equipotential lines calculated at the entrance ($z = 0.0$ mm). For comparison, the electric field above and below an infinite planar beam carrying line current J is
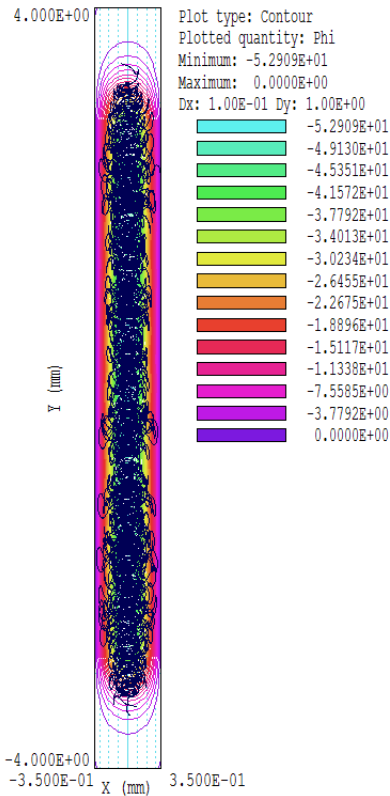
$$E_x = \pm \frac{J}{2\epsilon_0 \beta c}. \tag{1}$$

Figure 12: Particle orbits through the system projected to the x-y plane superimposed on the beam-generated potential distribution at $z = 0.0$ mm)

For $I = 3.1$ A and $\Delta y = 6.0$ mm, $J = 516.7$ A/m. The distance from the beam envelope to the grounded wall was $\Delta y = 0.20$ mm. The predicted potential at the envelope is $\phi = -40.0$ V. The theoretical voltage drop from the envelope to the axis is -15 V, so the expected minimum space-charge potential is $\phi \leq -55$ V, consistent with the calculated value of $\phi = -52.9$ V.

As a final task, I wanted to demonstrate how to transfer the planar beam distribution calculated in Sect. 2 to a magnetic transport calculation. There were three issues:

The PRT file represented only one quadrant of the beam.

Units of inches were used in gun calculation while the magnetic field solution had units of mm.

The origins of the axial coordinate systems for the two calculations were different.

To match the calculations, I used some existing functions of **GenDist** and added two utilities: the *Beam Section Tool* and the *Unit Conversion Tool.*
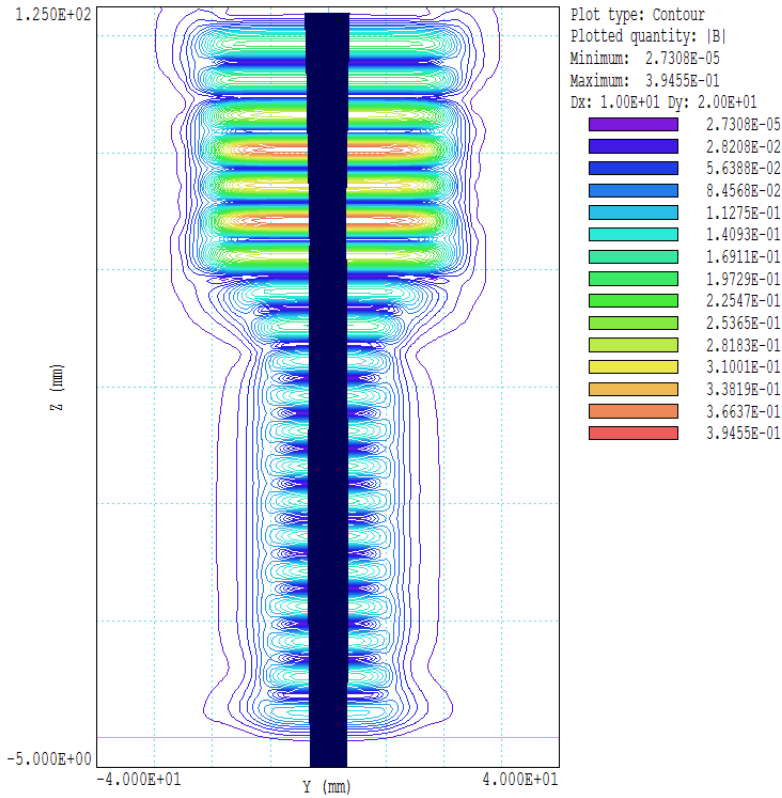
Figure 13: Long-direction confinement. Orbit projections and contours of $|\mathbf{B}|$ in the plane $x = 0.0$ for the input distribution from the gun calculation

One of the functions of the *Beam Section Tool* is to fill out the quadrants of three-dimensional distributions. The positions and momentum vectors are mirrored about symmetry axes. I applied the tool to `PLANARGUNR.PRT` to create `PLANARGUNR4.PRT` with 8336 model electrons. I next used the *Unit Conversion Tool* to transform the units from inches to mm. Here, **GenDist** determines the conversion factor and modifies the position vectors, leaving other particle parameters unchanged. The final step was to use the *Transform Distribution Tool* to move the particles from their exit position in the gun calculation ($z = 18.618$) to $z = -5.0$ mm.

I performed an **OmniTrak** calculation using the new *PRT* file as input to `TRANSPORT02.OIN`. The orbit projections in x-y were similar to those of Fig. 12 and again I observed 100% transport efficiency. Fig. 13 shows the beam dynamics in the long direction illustrating good confinement.